Synthesis and Characterization of Sol−Gel Hydrotalcites. Structure and Texture[†]

T. Lopez,*,[‡,§] P. Bosch,[‡] E. Ramos,[‡,§] R. Gomez,[‡,§] O. Novaro,[∥] D. Acosta,[∥] and F. Figueras[⊥]

Universidad Autónoma Metropolitana-Iztapalapa. Department of Chemistry, P.O. Box 55-534, México, D.F., 09340, México, Universidad de Guanajuato, Lazcurain de Retana s/n, Guanajuato, Guanajuato, México, IFUNAM, Circuito de la Investigacion, México, D.F., 01000, México, and Institut de Recherches sur la Catalyse du CNRS, 2 Av. A. Einstein, 69626 Villeurbanne Cedex, France

Hydrotalcites, which are anionic clays, have been synthesized by the sol−gel technique from magnesium ethoxide, aluminum tri-sec-butoxide, and aluminum acetylacetonate. Initially a colloidal solution is obtained which gels and is thermally stabilized. The local and average structure are studied comparing the electron microscopy results with the XRD patterns. One of the main features of these materials is the high specific area (around 150 m²/g), if compared with the natural hydrotalcites areas.

Introduction

Hydrotalcite is an anionic clay mineral whose general formula is $Mg_6Al_2(OH)_{16}CO_3 \cdot 4H_2O$. Hydrotalcites behave as basic materials[1−7] and are often used, for instance, as catalyst supports (Ziegler-Natta), as hydrogenation catalysts,[8] or as anionic exchangers.

Hydroytalcite presents a brucite-like structure. Mg^{2+} and Al^{3+} are octahedrally coordinated in a hydroxide Mg−Al sheet where the resulting positive charge excess is balanced by water molecules and anions as OH^-, Cl^-, CO_3^{2-}, NO_3^-, SO_4^{2-}, which define thus the basal (001) spacing.[9−11]

Hydrotalcites are stable up to 400 °C. At 200 °C, water molecules are lost and anhydrous hydrotalcite is obtained. At higher temperatures, CO_3^{2-} is removed and solids are partially hydroxylated; $Mg_6Al_2O_8(OH)_2$ is formed. If calcined at temperatures higher than 450 °C and up to 900 °C, MgO (periclase) and the spinel $MgAl_2O_4$ are irreversibly obtained. But, if calcined at around 500 °C, $Mg_6Al_2O_8(OH)_2$ is formed and, in the presence of water and carbonates, the original hydrotalcite is recovered.[12−14]

Conventionally, hydrotalcites are prepared by coprecipitation or by hydrothermal synthesis. In this report, the characterization of the texture of hydrotalcites synthesized by an alternative method, the sol−gel technique, is presented.

By conventional precipitation, the Mg/Al ratio in the solid obtained is limited to the range 1.5−3.0, and it was then attempted to increase this ratio by the sol−gel procedure. The characterization techniques were X-ray diffraction, nitrogen adsorption isotherm, BET method, and electron microscopy.

Experimental Section

HT-A Hydrotalcite. A 17.1-g portion of magnesium ethoxide (Alfa products, 99%) was dissolved in ethanol mixed with a small amount of HCl (Baker, 35% in water). Dissolution was refluxed at 80 °C with constant stirring. A second solution, composed of 1.93 mL of aluminum tri-sec-butoxide (Aldrich, 99%) and 20 mL of ethanol (Baker, 99.9%) was added. The pH of the mixture was maintained at 10 by adding NH₄OH (Baker, 33% NH₃ on water). Afterward, 2.7 mL of water was slowly added. The mixture (Mg/Al ratio = 13) was constantly stirred and refluxed until the gel was formed.

HT-B Hydrotalcite. A 11.4-g portion of Mg(OEt)₂ was dissolved in ethanol mixed with a small amount of HCl. The resulting solution was refluxed at 80 °C with constant agitation. A 4.86-g portion of aluminum acetylacetonate (Aldrich, 99%) was dissolved in 30 mL of acetone (Baker, 99%) and added to the refluxed solution, in order to obtain a Mg/Al ratio of 6. The pH of the mixture was maintained at 10 with NH₄OH. Afterward, 1.8 mL of water was added. The mixture was left in constant agitation and refluxed until the gel was obtained.

HT-C Hydrotalcite. A 17.1-g portion of Mg(OEt)₂ was dissolved in ethanol with HCl and refluxed at 80 °C with constant agitation. A solution obtained from 7.29 g of aluminum acetylcetonate and 30 mL of acetone was added (Mg/Al ratio of 6.6). The pH value was maintained at 10 using NH₄OH and 2.7 mL of water was added. The solution was maintained in reflux and constant agitation until gel formation.

All samples were dried at 70 °C for 24 h and then calcined at 150 and 300 °C.

Characterization

X-ray Diffraction. Diffractograms were obtained with a D500 Siemens diffractometer coupled to a copper anode tube using monocromatized Cu Kα radiation. Cell parameters were obtained using candle wax and corundum as internal standards. The candle wax has a diffraction

---

(1) Reichle, W. T. *J. Catal.* **1985**, *94*, 547.
(2) Reichle, W. T. *Solid State Ionics* **1986**, *22*, 135.
(3) Davis, R. J.; Derouane, E. G. *Nature* **1991**, *349*, 313.
(4) Davis, R. J.; Derouane, E. G. *J. Catal.* **1991**, *132*, 269.
(5) Pinnavaia, T. J. *Science* **1983**, *220* (4595). 365.
(6) Martin, K. K.; Pinnavaia, T. J. *J. Am. Chem. Soc.* **1986**, *108*, 541.
(7) Shannon, R. D. *Acta Crystallogr.* **1976**, *A32*, 751.
(8) Corma, A.; Fones, V.; Martin-Aranda, R. M.; Rey, F. *J. Catal.* **1992**, *134*, 58.
(9) Carrado, K. A.; Kostapapas, A: *Solid State Ionics* **1988**, *26*, 78.
(10) Dimotakis, E. D.; Pinnavaia, T. J. *Inorg. Chem.* **1990**, *29*, 2393.
(11) Miyata, S. *Clays Clay Miner.* **1985**, *28*, 370.
(12) Hernandez, M. J.; Ulibarri, M. A.; Cornejo, J.; Peia, M. J.; Serna, C. J. *Thermochim. Acta* **1985**, *94*, 257.
(13) Valcheva-Traykova, M. L.; Davidova, N. P.; Weiss, A. H. *J. Mater. Sci.* **1993**, *28*, 2157.
(14) Brindley, G. W.; Kikkawa, S. *Clays Clay Miner.* **1980**, *28*, 87.
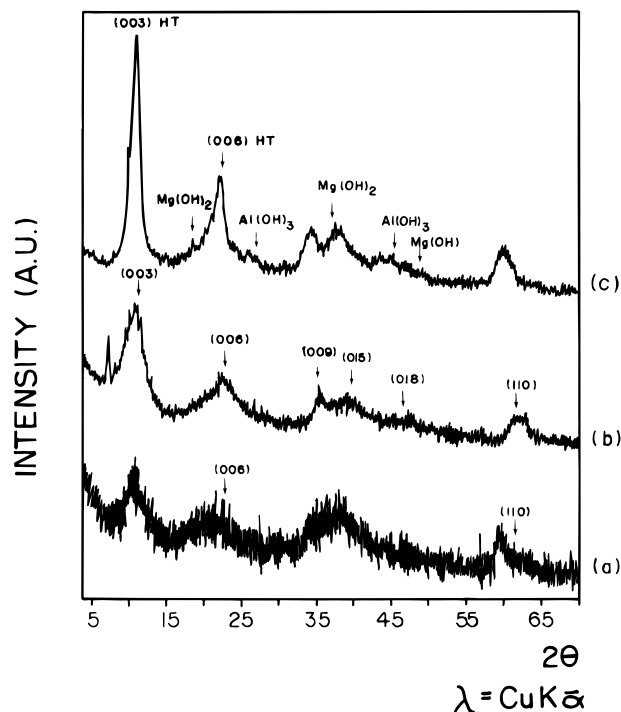
Figure 1. X-ray diffraction patterns of the fresh samples: (a) HT-A, (b) HT-B; (c) HT-C.
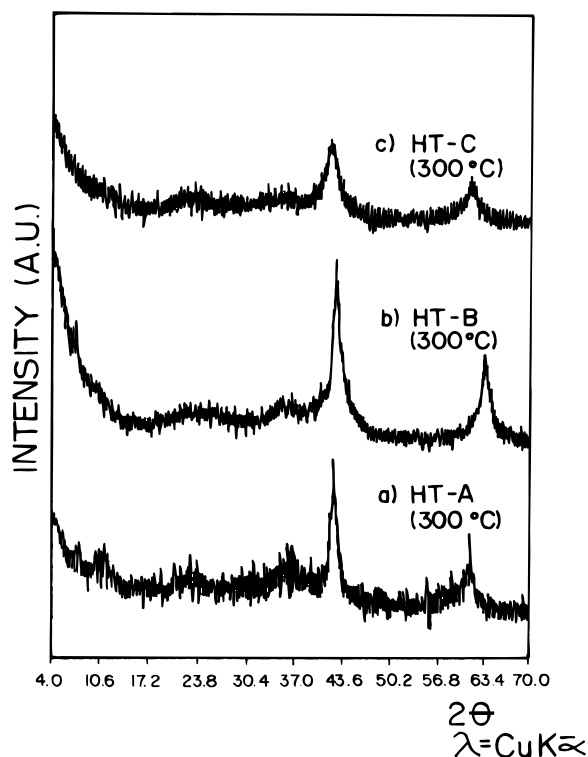

**Figure 2.** X-ray diffraction patterns of calcined samples at 300 °C: (a) HT-A; (b) HT-B; (c) HT-C.

peak at $2\theta = 2.05$ and corundum has two intense peaks at $2\theta = 25.5$ and $2\theta = 57.56$.

Electron Microscopy. Samples for scanning electron microscopy (SEM) were mounted on a conventional holder and covered with an electric conductor material. They were then observed in a JEOL 5200 electron microscope.

For conventional transmission electron microscopy (CTEM) studies, samples were ground in each case in an agate mortar. They were dispersed in distilled water in an ultrasonic bath. Some drops of solution were deposited
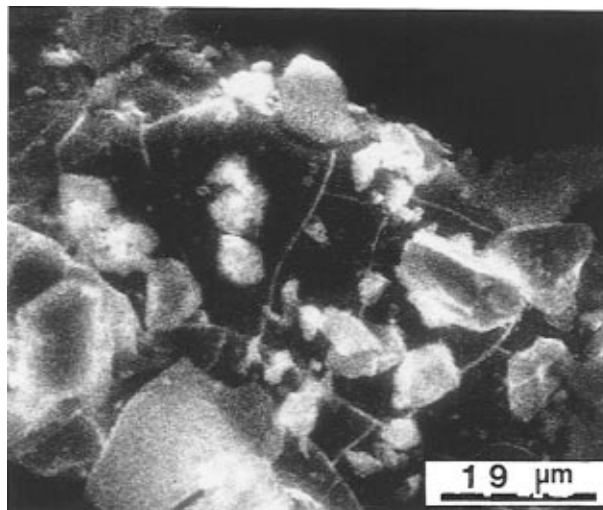
Figure 3. SEM images from HT-C treated at 300 °C. A big grain with cracks and an unidentified secondary phase can be observed.
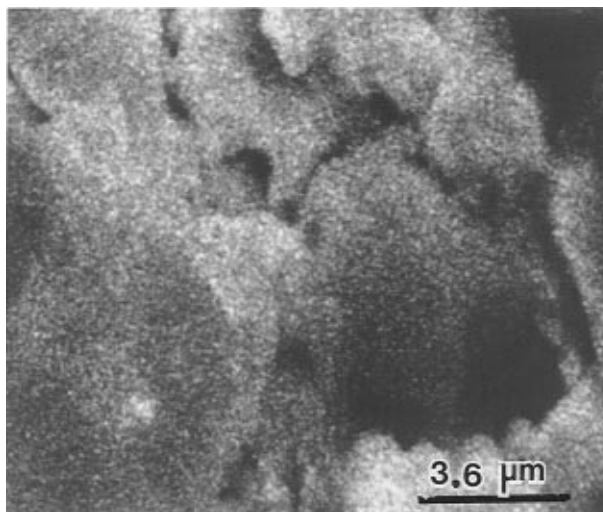
Figure 4. SEM image from HT-B treated at 150 °C where homogeneous granularity on the surface of big grains is observed.

on 200 mesh copper grids covered with a carbon film. Bright field images and selected area electron diffraction (SAED) patterns were obtained to study and characterize our samples.

BET Method. The adsorption isotherms of nitrogen were determined using an automatized micromeritics ASAP 2000. The BET surface area was obtained from these isotherms using the values of adsorption for P/P_0 in the range $0.05-0.25$. The distribution of pore sizes was determined using the classical BJH method, and the micropore volume was evaluated by the method of Dubinin, by extrapolation of the plot

$$\log v = \log v_0 + k(\log P/P_0)^2$$

to zero pressure.

Results and Discussion

X-ray Diffraction. X-ray diffraction patterns of the fresh samples (dried at 70 °C) are compared in Figure 1. The three samples are constituted by hydrotalcite (JCPDS card 22-0700). However, the degree of crystallization is different in each case, HT-A shows the broadest diffraction peaks and in HT-C the peaks are well-defined and sharp.
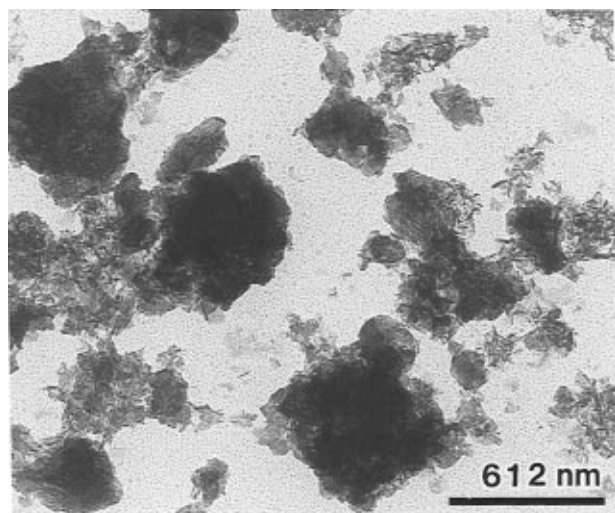
Figure 5. Bright field image where thick, dark detailed laminates of hydrotalcite are present.
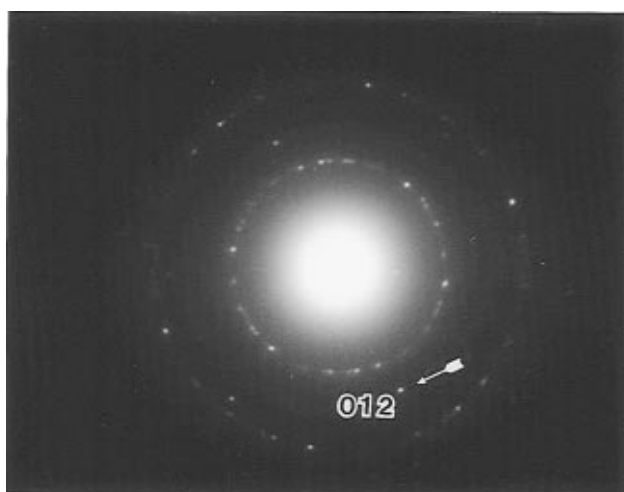

Figure 6. SAED pattern from HT-B treated at 150 °C. Polycrystalline hydrotalcite is identified.
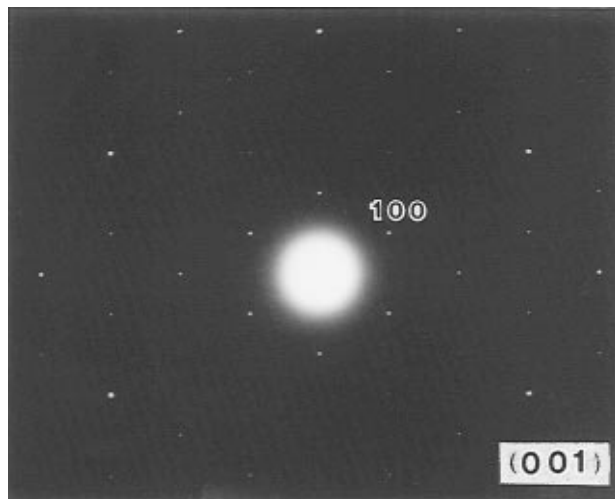

Figure 7. SAED pattern of crystalline hydrotalcite (HT-C, treated at 300 °C), presenting hexagonal structure.

The two hydrotalcites with the best crystallinity (HT-C and HT-B) present small peaks at $2\theta = 7.6$ attributed to some crystalline impurity.
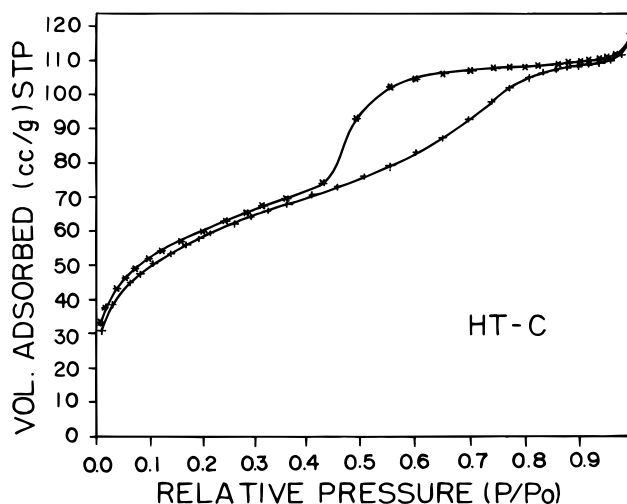
Cell parameters of HT-A were $a = 3.05$ Å and $c = 23.6$ Å. The cell parameters of HT-B and HT-C were $a = 3.07$ Å and $c = 23.71$ Å and $a = 3.06$ Å and $c = 23.34$ Å,
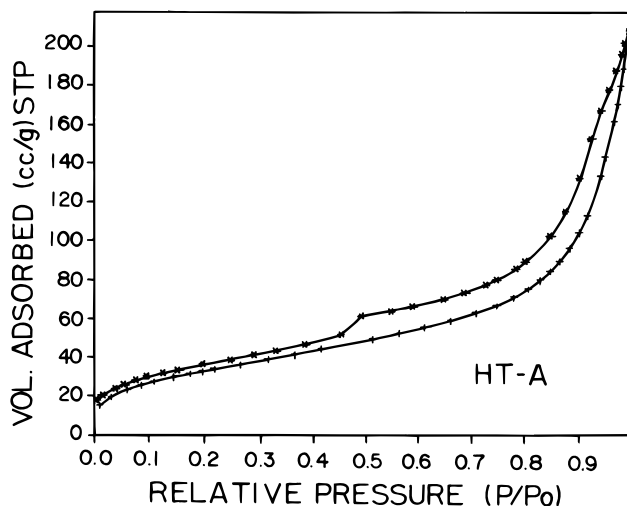
Figure 8. Nitrogen adsorption−desorption isotherm of HT-A.
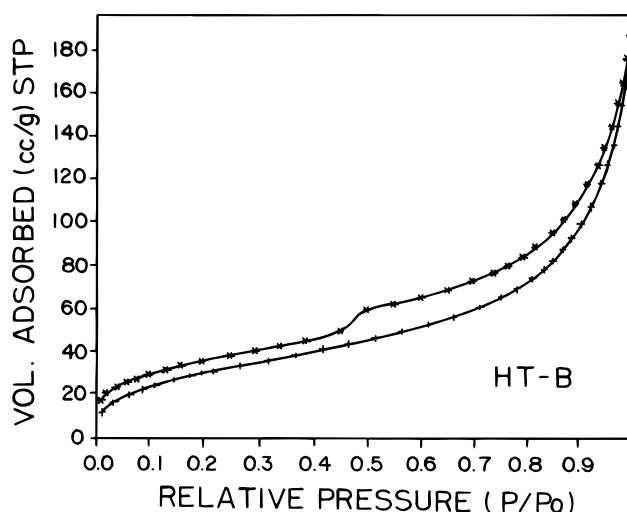
Figure 9. Nitrogen adsorption−desorption isotherm of HT-B.

Figure 10. Nitrogen adsoprtion−desorption isotherm of HT-C.

respectively. These values are in good agreement with those of the JCPDS card: $a = 3.102$ Å and $c = 23.404$ Å. The difference in the c value may be due to a variable hydration degree. Brindley and Kikkawa[15] have reported the values of the cell parameter of hydrotalcites as a function of the Al content. A Vegard law was observed

(15) Brindley, G. W.; Kikkawa, S. *Am. Mineral.* **1979**, *64*, 836.

up to a ratio Al/(Al + Mg) = 0.35. From this calibration curve, it can be concluded that this ratio in the solids prepared by sol−gel is 0.3 for sample A and 0.23 for samples B and C. The amount of Al incorporated to the lattice increases with the Al/Mg content of the solution. Since a solid with a Mg/Al ratio of 3.3 is produced from a solution with a Mg/Al ratio of 6, an excess of brucite must be formed. This brucite phase is formed in very small crystals or amorphous, since it is hardly detected by XRD.

If X-ray diffraction patterns of the 300 °C treated samples are compared, in Figure 2, the identified compounds are hydrotalcite (JCPDS card 22-0700) and periclase (JCPDS card 4-0829). Depending on the hydrotalcite content the samples may be ordered as follows: HT-A > HT-B = HT-C. In the HT-B and HT-C samples treated at 300 °C, hydrotalcite is, then, expected to be present as very small crystals undetected by X-ray diffraction.

Electron Microscopy. If samples are treated at 300 °C, SEM micrographs present big grains like those shown in Figure 3. They were commonly detected together with small aggregates of a secondary phase. In some cases, the surface of the grains presented roughness as shown in in Figure 4.

In all samples, by CTEM, plate configurations, Figure 5, were observed. By SAED, crystalline and polycrystalline materials, Figure 6, were identified: in most cases, hydrotalcite and periclase were detected in varying percentage. In HT-C small amounts of brucite were also found.

Figure 7 is the crystalline SAED pattern of HT-C treated at 300 °C hydrotalcite. This hexagonal pattern is characteristic of the hydrotalcite structure. Interplanar distances found from electron diffraction patterns analysis were compared with those reported for peryclase (MgO, ASTM card 4-0829), brucite (ASTM card 7-239), and hydrotalcite (ASTM cards 14-191 and 22-700) and the three compounds were detected in different samples (HT-A, HT-B, and HT-C). In all cases it was not found full coincidence between interplanar distances reported in ASTM cards and those derived from our electron diffraction patterns. In Figure 7, calculated d_{100} distance close to 0.305 nm, for instance, does not appear in ASTM cards, but after trial and error, calculations let us determine cell parameter *a* close to one reported, $a = 0.307$ nm, for hydrotalcite hexagonal structure. This result confirms the hypothesis presented in the X-ray diffraction paragraph. Crystalline hydrotalcite is indeed present in this sample.

BET Surface Areas. The adsorption−desorption isotherms are presented in Figures 8, 9, and 10. They all show an hysteresis loop at low relative pressures <0.4,

Table 1. Surface Area and Porosity Determined by N₂ Adsorption

samples[a]	BET surface area (m²/g)	micropore area (m²/g)	total pore volume (cm³/g)	micropore volume (cm²/g)
HT-A	121		0.22	<0.01
HT-B	110		0.20	≤0.01
HT-C	211	54	0.17	0.02

[a] All the samples were evacuated at 25 °C.

which may be attributed to diffusional resistance introduced by the presence of very small pores which reach equilibrium with the gas phase only for very long times. This phenomenon remains however limited and does not induce a big error in the values of the surface areas of the materials. These results were expected given the hydrotalcite structure. In HT-C, as shown in Table 1, the micropore volume is higher than those of in the HT-A and HT-B samples. Therefore in HT-C, the surface area value is the highest. This result has to be attributed to the higher aluminum content in the gelation reaction. Magnesium atoms are substituted by aluminum atoms, as shown by XRD, and the amount of hydrotalcite is higher. The HT-C sample is, hence, more ordered than the two other samples. This remark is confirmed by the crystallite size determined in XRD. In principle two parameters determine the breadth of XRD peaks the presence of defects and size of crystals. Hydrotalcite is a laminar structure in which the (001) spacing is determined by the nature of anions balancing the charge. It is then expected that the stacking of the sheets is regular and the size of the crystals in the (001) direction determins the breadth of the XRD lines. In the other directions the random distribution of Al ions in the brucite lattice may be a second source of broadening of the peaks. The particle size was then evaluated in the (001) direction using the (003) reflection, and the sample HT-C showed the larger crystallite (114 Å).

Conclusions

The parameters in the sol−gel synthesis of hydrotalcites determine the structure and the texture of the obtained materials. Although aluminun precursor (aluminum alkoxide or aluminum acetylacetonate) and aluminum content were varied, in all cases hydrotalcite was obtained, mixed with a dispersed Mg(OH)₂ phase. For Mg/Al ratios close to 6 in the solution (HT-C) a higher surface area hydrotalcite is obtained.